

2019-03-07

Evaluation of tensile properties of fibers extracted from banana peels

Ferrante, A

<http://hdl.handle.net/10026.1/13450>

10.1080/15440478.2019.1582000

Journal of Natural Fibers

Taylor & Francis

All content in PEARL is protected by copyright law. Author manuscripts are made available in accordance with publisher policies. Please cite only the published version using the details provided on the item record or document. In the absence of an open licence (e.g. Creative Commons), permissions for further reuse of content should be sought from the publisher or author.

Evaluation of Tensile Properties of Fibers extracted from Banana Peels

Achille Ferrante, Carlo Santulli

Università di Camerino, School of Architecture and Design, 63100 Ascoli Piceno, Italy

and John Summerscales

University of Plymouth, Faculty of Science and Engineering, Plymouth PL4 8AA UK

ABSTRACT

Tensile properties of banana fibres extracted from the peel of the fruit of the Cavendish sub-group were studied. A total of 43 fibres were manually extracted from the peel of green bananas, measuring five diameters from each fibre. The fibres were examined under the optical microscope up to a 50x magnification and their cross-sectional area (CSA) was observed. Tensile tests were conducted on the extracted banana fibres and Young's modulus was calculated using area apparent from microscopy observations, then calculating a fibre area correction factor (FACF) to reduce the relevant error. Geometry and extent of the lumen was also measured.

KEYWORDS

Banana peels; tensile strength; fibre extraction; section measurement

INTRODUCTION

Banana peels are an abundant agro-waste: in practice, around one ton of waste is produced for every ten tons of bananas, hence around 10% (FAO 2013). A number of uses have been proposed for this waste: for example, since it is suitable for feeding of animals, such as cows, being rich in starch, sugar and potassium, it was proposed as dietary fibre (Emaga et al. 2007). On the other side, also more added value applications have been attempted: the possibility to extract nanocellulose fibres has been investigated (Tibolla, Pelissari and Menegalli 2014). Also, other parts of the banana plant, such as the pseudo-stem, proved able to supply cellulose fibres with sufficient tensile strength, and therefore adapted to the production of fibre boards, which could also be the case for banana peels (Mohapatra, Mishra and Sutar, 2010).

Some uses, which have been envisaged for banana peels, would require their introduction in a biopolymer matrix as reinforcement. In particular, some applications that were suggested, are in the absorption of heavy metals (Annadurai, Juang and Lee 2002), such as lead and cadmium (Anwar et al., 2010) or chromium (Memon et al. 2009), and as a replacement for asbestos for brake pads (Idris et al. 2015).

The use of banana peels as the reinforcement for biopolymers, most possibly in the form of random fibres would require an accurate measurement of their section, to determine the tensile stress and Young's modulus. The difficulty is due to the fact that the section includes a lumen of complex shape and has geometry far removed from a circular one. Section measurement on plant fibres using image analysis from microscopic observation has been carried out on jute (Virk, Hall, and Summerscales 2010) sisal and flax fibres (Idicula et al. 2005). In this instance, the cross-sectional area of the fibres is assumed circular, then correction factors need to be calculated (Virk, Hall, and Summerscales 2012).

In this work, fibres were extracted from banana peels by manual stripping, and their apparent diameter was measured. Following this, tensile tests were performed on the fibres, measuring then the section of fibres to allow correcting the mechanical stress results with respect to the assumption of a circular shape. The main idea of this study is to prove whether fibres yield sufficient properties to be introduced in biodegradable matrices to exploit their capabilities as far as heavy metal absorption potential is concerned.

MATERIALS AND METHODS

Diameter measurements

Peels of green, unripe bananas were considered for the extraction of the fibres. The variety of bananas analysed was the Cavendish, imported from Cameroon and Dominican Republic. A total of 43 fibres were extracted: after the extraction, the fibres were dried in oven at 70°C for 60 minutes, to prepare them for measurement. The average length of the banana fibres (BF) stripped out from the peels was between 150-200 mm. The BFs were then mounted on the test cards for the tensile tests based on Grafil Test 101.13 (Grafil Test Methods, Courtaulds Ltd, 1980). The fibres were secured on the test card using SURELOC Adhesive CA 1500, applied at both the ends for each specimen, which ensured a 50 mm window for measurement, as illustrated in Figure 1.

Each specimen was observed under the microscope for the diameter measurements. The fibres were examined using an Olympus BX60MF optical microscope (Serial number 6M04733) at a 50x magnification and the diameters were measured using the image-analysis software Olympus Stream Motion. Measurements at 5%, 25%, 50%, 75% and 95% (respectively d1, d2, d3, d4 and d5) of the 50 mm window have been noted. The measure of 195 diameters was recorded, since a few of them proved unsuccessful (20 over a total of 215 attempted).

The measurement of the BF apparent diameter was calculated by measuring the maximum chord visible on the fibre once it was properly magnified, as shown in Figure 2. An irregular shape of the section was assumed after this first examination. In some points, the fibres were twisted on themselves into a spiral as shown in Figure 3. This has meant that the section was not constant along the fibre and that some imperfection could have affected the mechanical properties.

Tensile testing

For tensile testing, a gauge length of 50 mm was considered and 30 fibres were tested, those which did not break before testing. The test cards were cut in the middle before each specimen was tested as shown in Figure 4. Tests were carried out on BF of 113,90 µm average diameter, using an Instron 3345 K1669 universal testing machine with an Instron 10N load cell (model 2519-101, serial number - 64560) at constant testing speed of $0,5 \cdot 10^{-3} \text{ m min}^{-1}$, which needed to be considered into evaluating the results.

Cross-sectional area measurement

BFs were prepared for the cross-sectional area (CSA) observation under the microscope. The extraction and drying process followed was the same described for the preparation of the specimens for the tensile testing phase. This experiment aimed to fix enough fibres vertically and as accurately as possible, to look properly at the CSA under the microscope.

The specimen for the CSA analysis was mounted by fixing 4 small plates of transparent poly(methylmetacrylate) (PMMA) (maximum length 40 mm, maximum width 15 mm and around 1 mm thickness) on the base of a round plastic mould with a diameter of 40 mm, as shown in Figure 5. 25 BF were mounted on the plates and secured with SURELOC Adhesive CA 1500 for the alignment. Then, the plates with the BF were cast into epoxy resin. After the curing time, the specimen was ready for grinding and polishing.

The specimen was ground flat in stages on grit paper and then polished with MetaDi™ Monocrystalline diamond suspension with 6 µm, then 1µm fineness. Finally, the CSA of each fibre was examined using an Olympus BX60MF optical microscope (Serial number 6M04733) and the section was clearly not circular as assumed before (Figure 6). All the shapes observed were irregular and all different from each other.

In order to measure the true cross-sectional area (tCSA), the images were converted into binary format (black and white) and processed using the public domain software ImageJ (version 1.51j8). Maximum chord and tCSA were measured after proper scaling of each image, as shown in Figure 7. A Coefficient of Variation (CoV), defined as the ratio (in percent) between the standard deviation of values and the average value of apparent areas is calculated. Moreover, a Fibre Area Correction Factor (FACF) is also calculated, as the ratio between two areas: the former measured under the microscope, namely the *apparent area*, resulting from the diameter measurement, and the latter, namely the *definitive area*, resulting from the cross-sectional measurement (Virk, Hall and Summerscales 2012). The definitive area also excludes the lumen area from measurement.

RESULTS AND DISCUSSION

Results of diameter measurements

The average diameters were calculated for each specimen as shown in Figure 8. In Table 1 are reported the results obtained from the tensile testing of 30 specimens of BF.

The maximum load at failure (P') recorded was from sample number 028 and it was of 1.85 N. Extension for Young's Modulus calculation (Δ) was extracted from the CSV (comma-separated values) dataset looking at the linear section between 0.1 and 0.2 N for each sample tested (Figure 9). The extension at break (ε) divided by the gauge length (l) of 50 mm was used for the strain at break (ε').

Stress at break (σ') was calculated and Young's Modulus calculations were based on the diameters measured before the tests when the CSA was assumed to be a circle. Equations 1, 2 and 3 show how Young's Modulus (E), strain at break (ε') and stress at break (σ') were calculated.

$$E = \frac{F}{A} \cdot \frac{l}{\Delta} = \frac{F}{\pi \cdot \frac{d^2}{4}} \cdot \frac{l}{\Delta} \quad (1)$$

$$\sigma' = \frac{P'}{A} = \frac{P'}{\pi \cdot \frac{d^2}{4}} \quad (2)$$

$$\varepsilon' = \frac{\varepsilon}{l} \quad (3)$$

where E was expressed in GPa, σ' in MPa and ε' as percentage value.

Fibre area correction factor

Random samples of BF were chosen for the FACF calculation (Virk, Hall and Summerscales 2012). The correction factor was calculated dividing the apparent CSA ($A_{app(c)}$) based on the maximum chord (C_{max}) measured on ImageJ and assumed as diameter, by the definitive CSA (A_{def}). The A_{def} was calculated by subtracting the lumen area (A_{lumen}) from the true area (A_{true}) measured on ImageJ from the binary images of the cross-sections (Figure 10). ImageJ calculation is performed by setting a known distance, which the software converts into binary pixels.

The results of the areas calculation are given in Table 2. A comparison of the different areas is shown in Figure 11, which highlights that CSA is significantly overestimated from the first calculation, based on the apparent diameter measured from side-view observation of the BF. A further overestimation, though smaller, is obtained by not considering the lumens. Thus, by measuring and selecting the right CSA (A_{def}), a correct estimation of the FACF can be carried out.

As the consequence of the above considerations, an average correction factor (FACF), equal to the ratio between the average apparent cross-sectional area and the average definitive cross-sectional area equal to 2.982 was calculated using Equations 4, as follows:

$$FACF = \frac{A_{app(c)}}{A_{def}} \quad (4)$$

The accuracy of FACF calculation is increased with the number of fibre measurements.

Discussion

The results, first those based on the apparent value of fibre section, then corrected by the application of the FACF, are reported in Table 3.

In literature, by calculating a FACF it was possible to correct the prediction of the mechanical properties using the Rule of Mixtures (RoM) of a hypothetical composite with BF as reinforcement in a volume fraction between 0.05 and 0.20 (Virk, Hall and Summerscales 2012). Based on the aforementioned study, the same calculation is repeated from the values presently obtained. In particular, in Equation 5, κ is the FACF, η_d is the fibre diameter distribution factor (assumed as 1), η_l is the fibre length distribution factor (assumed as 1), η_o is the fibre orientation distribution factor (random orientation), V_f is the volume fraction of the fibre (0.05-0.20), E_f is the Young's modulus, V_m is the volume fraction of the matrix and E_m is the Young's modulus of the matrix.

$$E_c = \kappa \eta_d \eta_l \eta_o V_f E_f + V_m E_m \quad (5)$$

From a morphological point of view, after a careful observation, the cross-sections were separated in two groups: quasi-circular and elongated: these are reported in Figure 12. For the first group of quasi-circular fibres the evaluation of an average diameter to measure real cross-sectional can possibly offer a realistic idea, whereas for the second group of elongated fibres it cannot. Other cases are between the two, therefore it is uncertain whether an approximation with the average diameter does offer quite accurate results, since it needs also to be considered that the section is variable across the fibre length.

In Figure 13 two samples are depicted, belonging each one to the group of quasi-circular or elongated fibres and in this case showing also the lumen areas, which are distributed across the whole section and not concentrated in their centre. Measurements of the lumens were taken and listed in Table 4, from which an average value of 15% of lumen for each BF was observed, considering that lumen sub-areas of less than $2 \mu\text{m}^2$ are not detected by the software.

After performing this calculation, the point of the study was to see how sections and stiffness of banana peel fibres compared with data for other similar fibres present in literature, which are summed up in Table 5. Data obtained from this work are presented in bold. It can be seen that the stiffness values for banana peels are considerably lower than from data in literature. This is to be expected as it is a material obtained from fruit waste, rather than from the stem or the leaves of the plant, which are much larger and stiffer structures.

CONCLUSIONS

The study carried out has revealed part of the mechanical properties of the fibres extracted from the peel of the bananas, usually extracted from the leaves or from the bark of the banana plant. An accurate observation of the cross-sections and of the lumen was carried out and the data obtained from the analysis were compared with data from other natural fibres. Further studies would regard the mechanical properties of a composite material with banana fibres extracted from the peel of the fruit as reinforcement.

REFERENCES

- Alves Fidelis, M. E., T. V. Castro Pereira, O. d. F. Martins Gomes, F. De Andrade Silva and R. D. Toledo Filho. 2013. The effect of fiber morphology on the tensile strength of natural fibers. *Journal of Materials Research and Technology* 2(2):149-157.
- Annadurai, G., R. S. Juang and D. J. Lee. 2002. Adsorption of heavy metals from water using banana and orange peels. *Water Science and Technology* 47(1):185-190.
- Anwar, J., U. Shafique, W. Zaman, M. Salman, A. Dar and S. Anwar. 2010. Removal of Pb(II) and Cd(II) from water by adsorption on peels of banana. *Bioresource Technology* 101:1752-1755.
- Emaga, T. H., R. H. Andrianaivo, B. Wathelet, J. T. Tchango and M. Paquot. 2007. Effects of the stage of maturation and varieties on the chemical composition of banana and plantain peels. *Food Chemistry* 103:590-600.
- FAO, Food and Agriculture Organization of the United Nations. 2013. Food Balance Sheets: Bananas Production and Losses. FAOSTAT Statistics Database.
- Grafil Test Methods (reference 101.13). March 1980. Courtaulds Limited, Coventry.
- Idicula, M., S. K. Malhotra, K. Joseph and S. Thomas. 2005. Dynamic mechanical analysis of randomly oriented intimately mixed short banana/sisal hybrid fibre reinforced polyester composites. *Composites Science and Technology* 65:1077-1087.
- Idris, U. D., V. S. Aigbodion, I. J. Abubakar and C. I. Nwoye. 2015. Eco-friendly asbestos free brake-pad: Using banana peels. *Journal of King Saud University - Engineering Sciences* 27:185-192.
- Joseph, S., M. S. Sreekala, Z. Oommen, P. Koshy and S. Thomas. 2002. A comparison of the mechanical properties of phenol formaldehyde composites reinforced with banana fibres and glass fibres. *Composites Science and Technology* 62:1857-1868.
- Jústiz-Smith, N. G., G. Junior Virgo and V.E. Buchanan. 2008. Potential of Jamaican banana, coconut coir and bagasse fibres as composite materials. *Material Characterization* 59:1273-1278.
- Kulkarni, A. G., K. G. Satyanarayana, P.K. Rohatgi and K. Vijayan. 1983. Mechanical properties of banana fibres (*Musa sapientum*). *Journal of Material Science* 18:2290-2296.
- Memon, J. R., S. Q. Memon, M. I. Bhanger, G. Z. Memon, A. El-Turki and G.C. Allen. 2008. Characterization of banana peel by scanning electron microscopy and FT-IR spectroscopy and its use for cadmium removal. *Colloids and Surfaces B: Biointerfaces* 66:260-265.
- Memon, J. R., S. Q. Memon, M. I. Bhanger, G. Z. Memon, A. El-Turki, K.R Hallam and G. C. Allen. 2009. Banana peel: A green and economical sorbent for the selective removal of Cr(VI) from industrial wastewater. *Colloids and Surfaces B: Biointerfaces* 70:232-237.
- Mohapatra, D., Mishra, S., Sutar, N. 2010, Banana and its by-product utilisation: a review, *Journal of Scientific and Industrial Research* 69: 323-329.
- Oksman, K., L. Wallstrom, L. A. Berglund and R. D. Toledo Filho. 2002. Morphology and Mechanical Properties of Unidirectional Sisal-Epoxy Composites. *Journal of Applied Polymer Science* 84:2358-2365.
- Pothan, L. A., S. Thomas and N. R. Neelakantan. 1997. Short Banana Fiber Reinforced Polyester Composites: Mechanical, Failure and Aging Characteristics. *Journal of Reinforced Plastics and Composites* 16(8):744-765.
- Pothan, L. A., Z. Oommen and S. Thomas. 2003. Dynamic mechanical analysis of banana fiber reinforced polyester composites. *Composites Science and Technology* 63:283-293.

- Rao, M. M., K., . K. Mohana Rao, and A. V. Ratna Prasad. 2010. Fabrication and testing of natural fibre composites: vakka, sisal, bamboo and banana. *Materials and Design* 31:508–13.
- Sapuan, S. M., A. Leenie, M. Harimi and Beng. Y.K. 2006. Mechanical properties of woven banana fibre reinforced epoxy composites. *Materials and Design* 27:689-693.
- Thomason, J. L., J. Carruthers, J. Kelly and G. Johnson. 2011. Fibre cross-section determination and variability in sisal and flax and its effects on fibre performance characterisation. *Composites Science and Technology* 71:1008-1015.
- Tibolla, H., F. M. Pelissari and F.C. Menegalli. 2014. Cellulose nanofibers produced from banana peel by chemical and enzymatic treatment. *LWT - Food Science and Technology* 59:1311-1318.
- Virk, A. S., and J. Summerscales, 2009. Multiple Data Set (MDS) weak-link scaling analysis of jute fibres, *Composites Part A: Applied Science and Manufacturing* 40: 2009, 1764–1771.
- Virk, A. S., W. Hall and J. Summerscales. 2010. Physical Characterization of Jute Technical Fibers: Fiber Dimensions. *Journal of Natural Fibers* 7:216-228.
- Virk, A. S., W. Hall and J. Summerscales. 2012. Modulus and strength prediction for natural fibre composites. *Materials Science and Technology* 28 (7):864-871.

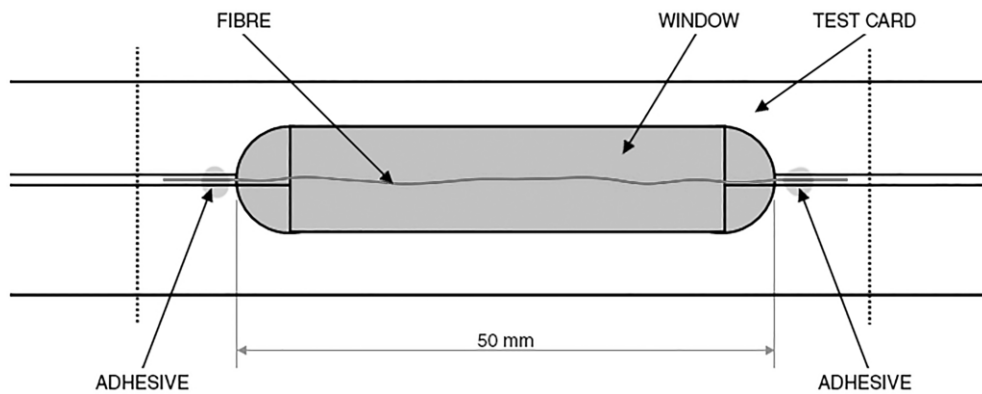


Figure 1: Single fibre mounted on the test card.

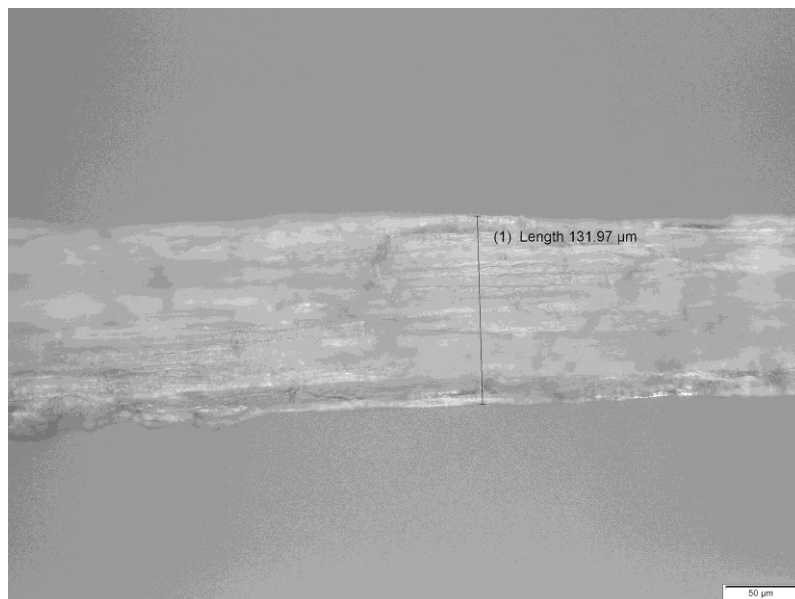


Figure 2: Measurement of the diameter of the fibre.

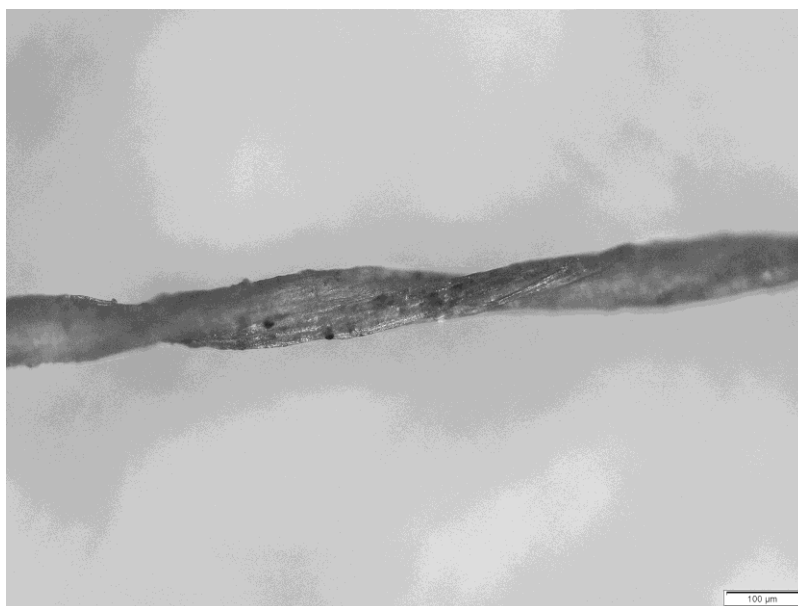


Figure 3: Fibre twisted on itself into a spiral.

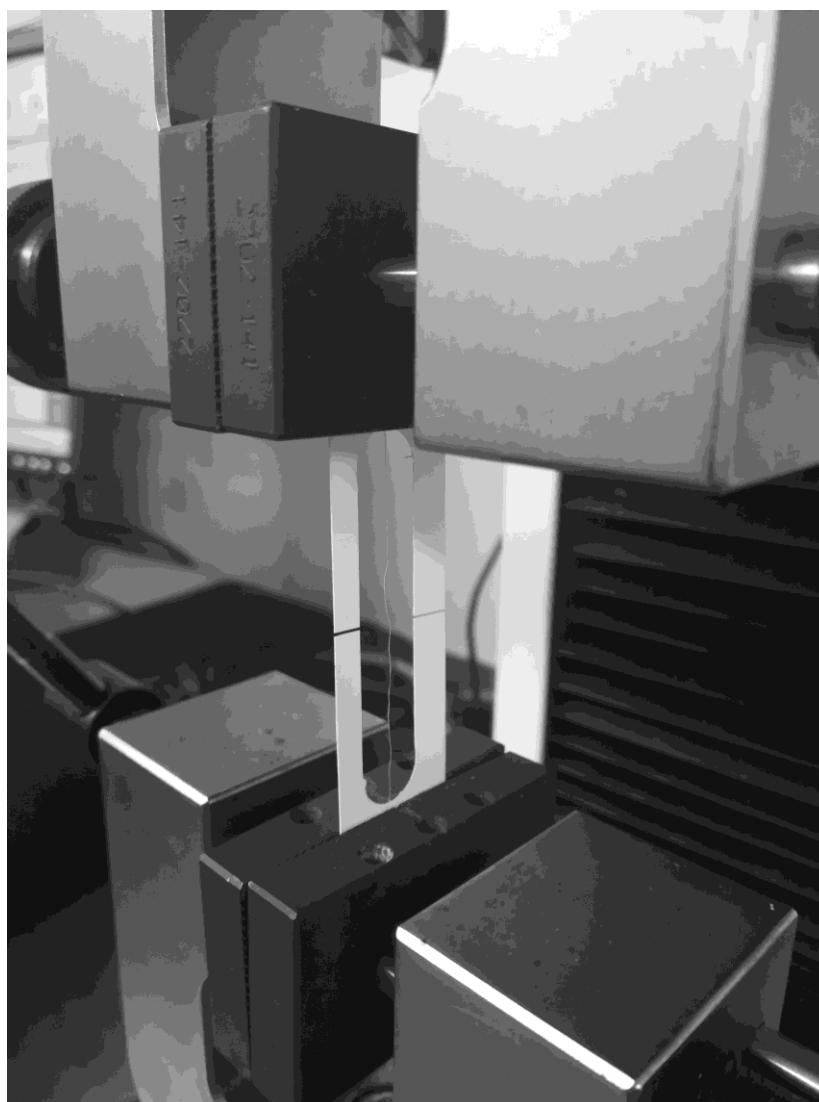


Figure 4: Test card cut at the middle and secured between the grips.

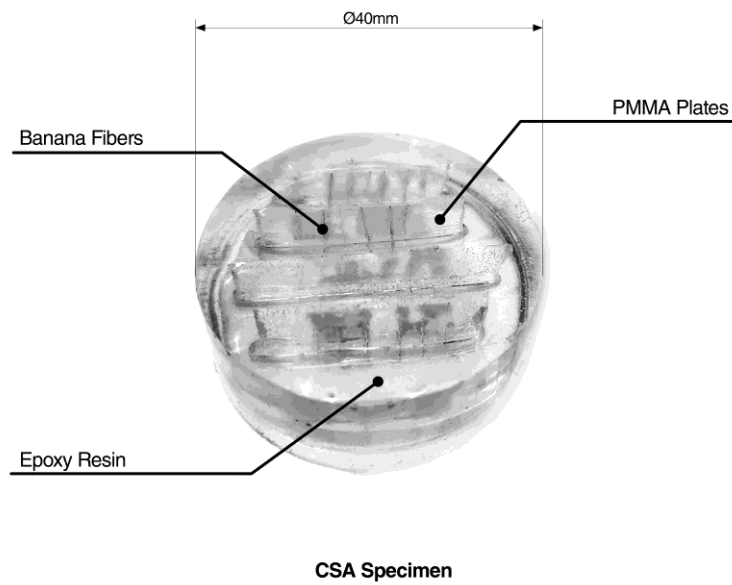


Figure 5: CSA epoxy specimen.

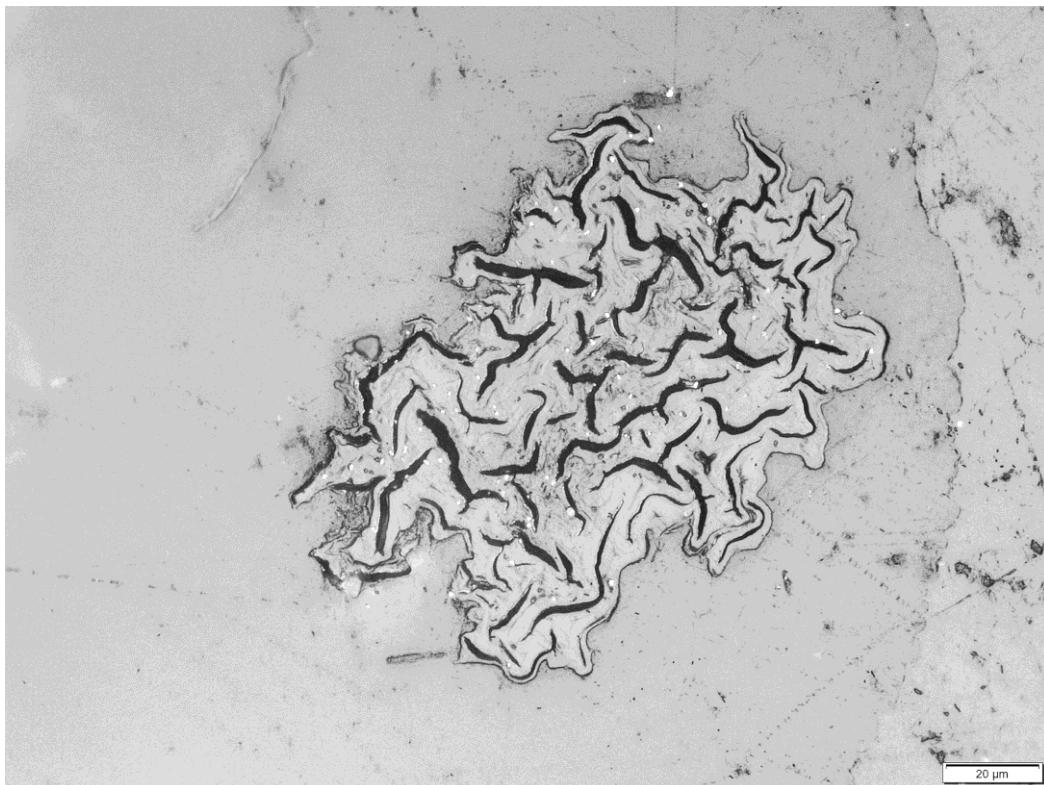


Figure 6: True cross-sectional area of one banana fibre.

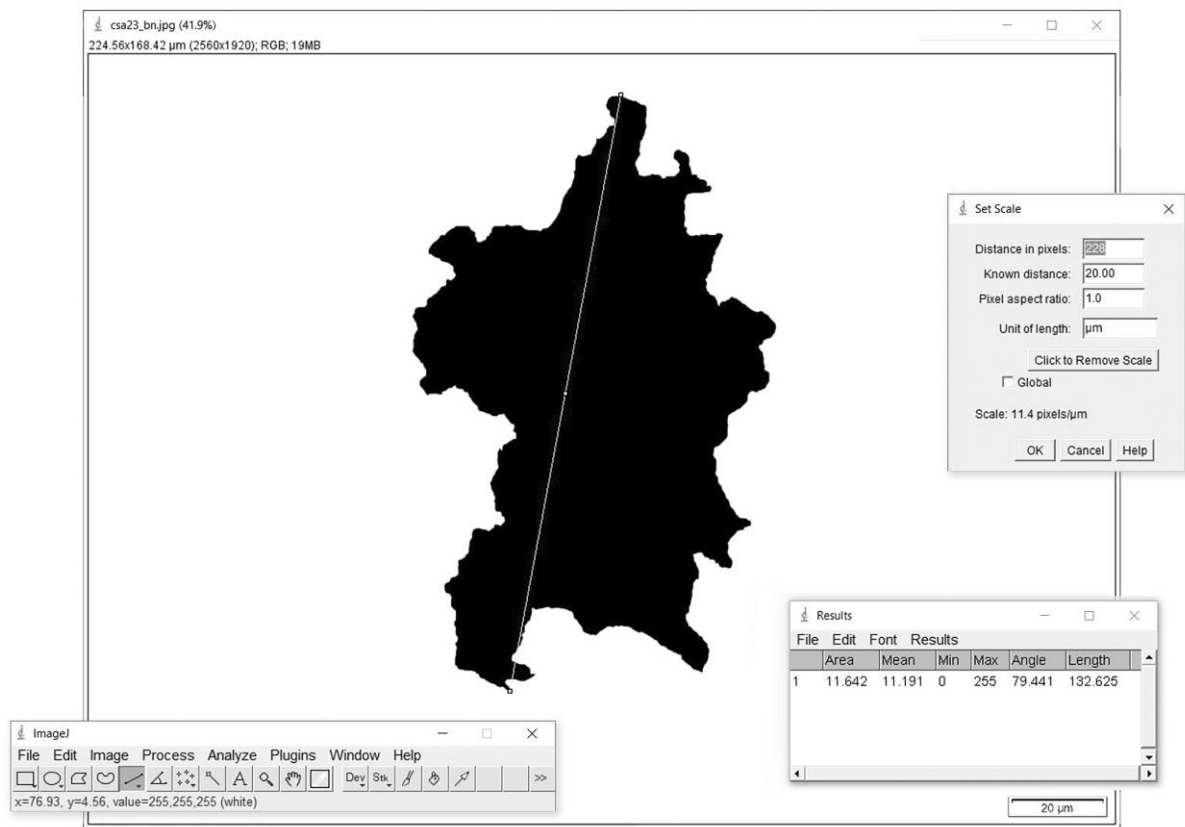


Figure 7: Image processing with ImageJ software.

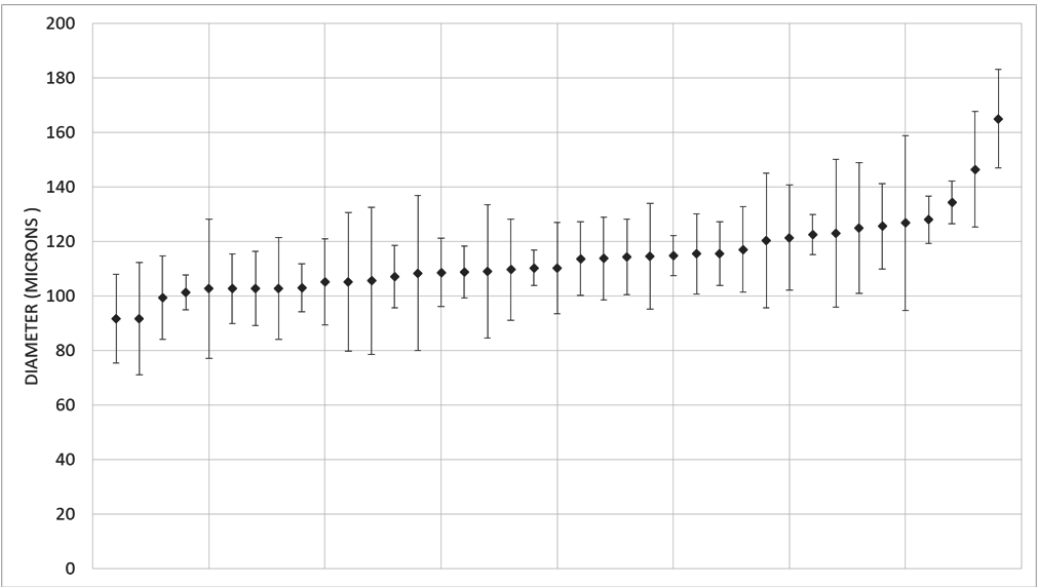


Figure 8: Average diameters of BFs.

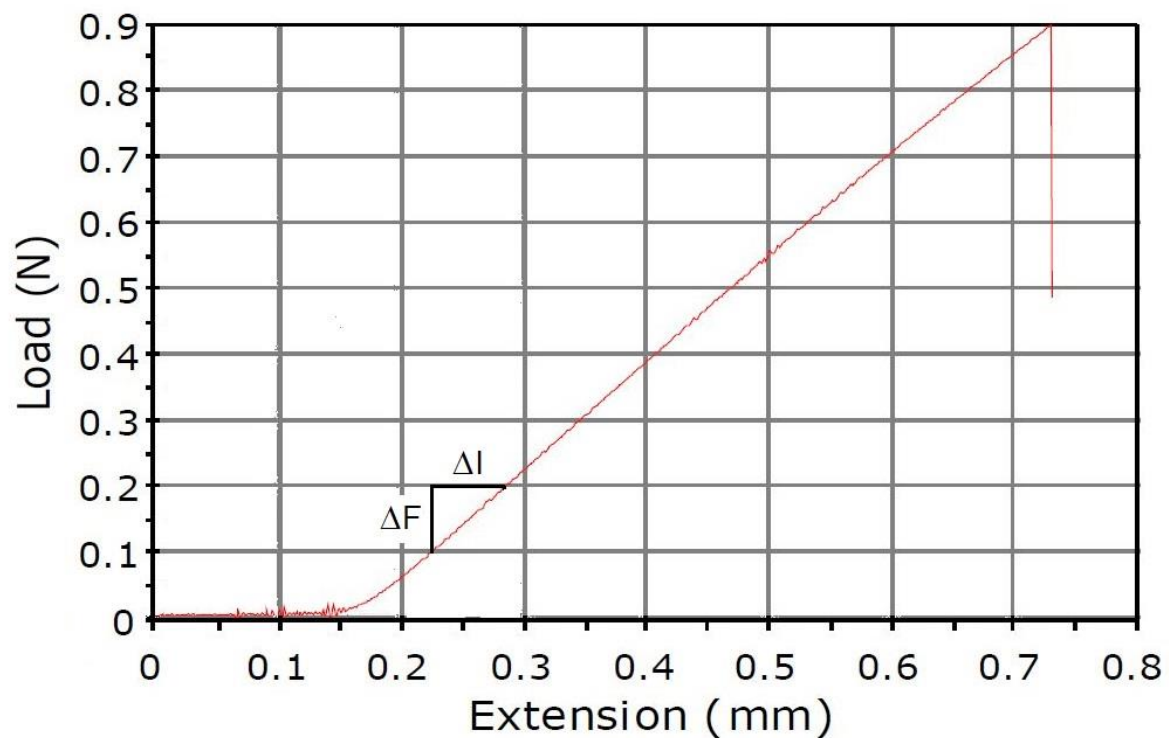


Figure 9: Young's modulus measurement from linear part of tensile curve

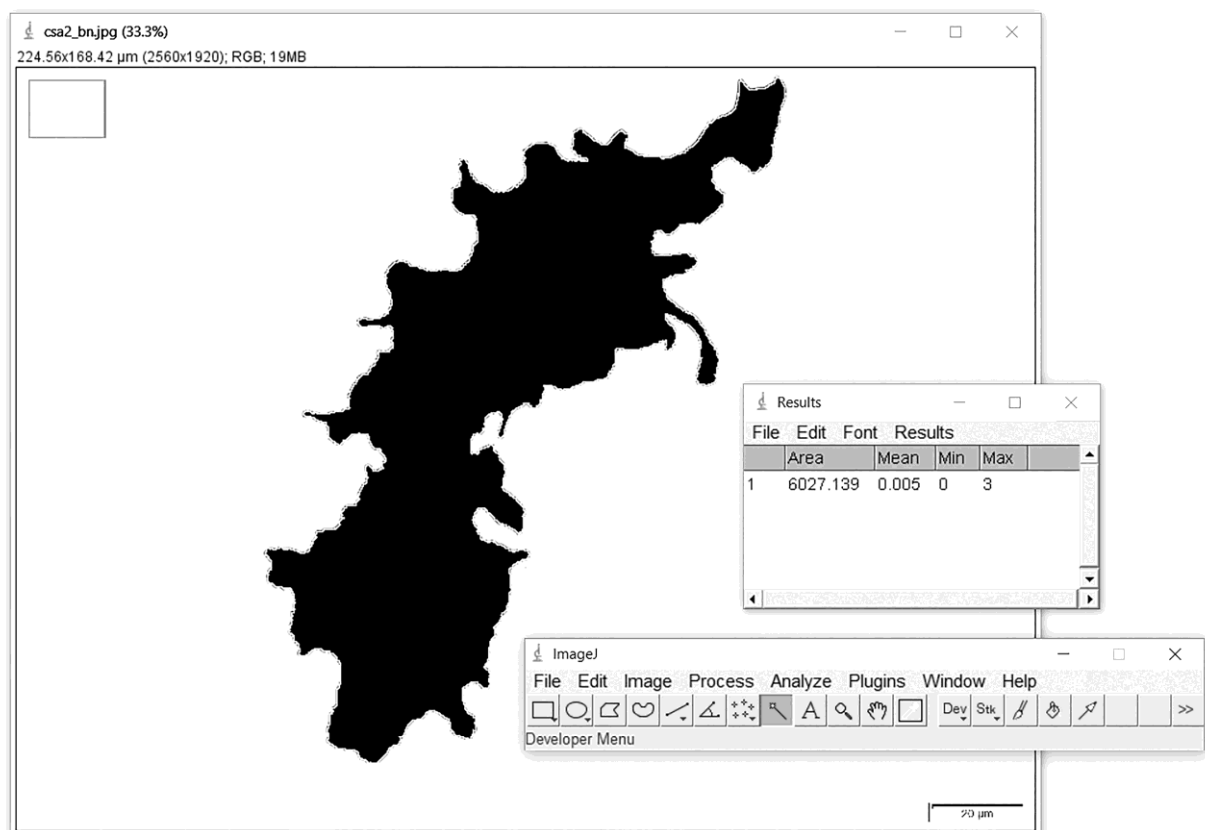


Figure 10: Area calculation from binary image of the cross-section

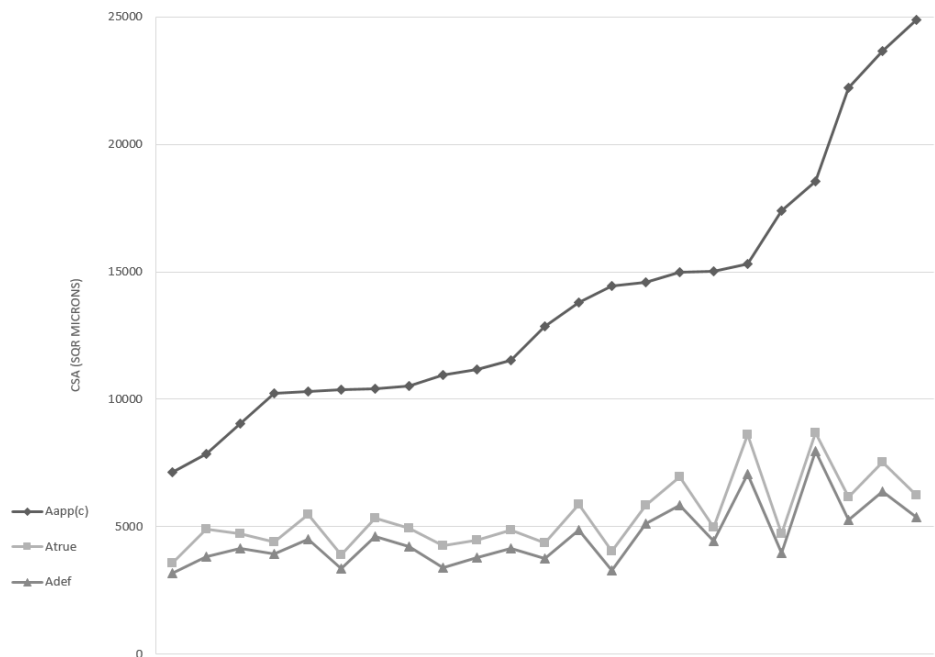


Figure 11: Comparison of the different areas on the same fibers





















Quasi circular	Undefined	Elongated
		
		
		
		
		
		
		
		
		
		

Figure 12: Fibre sections classified according to their shape

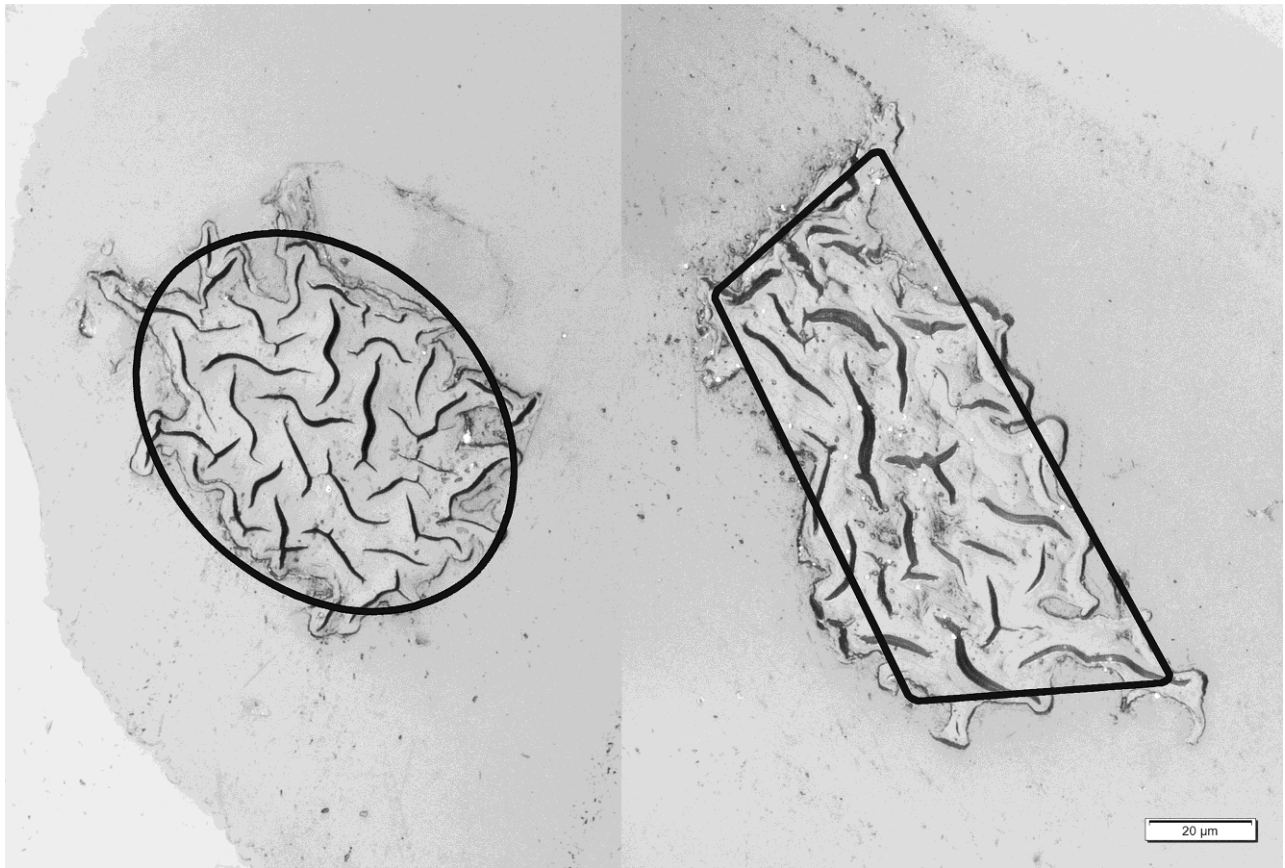


Figure 13: Sample of one quasi-circular and one elongated fibre, showing also the distributed lumen extension

Table 1: BF tensile tests results

	σ' (MPa)	ϵ' (%)	E (GPa)
Mean	91.19	1.71	7.35
StDevP	27.63	0.57	1.95
CoV (%)	30.30	33.12	26.56

 σ' : Stress at break ϵ' : Strain at break

E: Young's Modulus

StDevP: Standard Deviation

CoV: Coefficient of Variation

Table 2: Banana fibres CSA results

	C_{\max} (μm)	$A_{\text{app(c)}}$ (μm^2)	A_{true} (μm^2)	A_{lumen} (μm^2)	Lumen %	A_{def} (μm^2)
Mean	130.70	13791	5429	805	14.92	4624
StDevP	21.85	4734	1366	252	3.22	1210
CoV (%)	16.72	34.33	25.16	31.29	21.58	26.17

 C_{\max} (μm): Maximum chord of the fiber $A_{\text{app(c)}}$ (μm^2): Apparent area based on the chord A_{true} (μm^2): True area calculated on ImageJ binary images of the CSA A_{lumen} (μm^2): Lumen area of the fiber calculated on ImageJ binary images of the CSALumen %: Lumen percentage in the A_{true} A_{def} (μm^2): Definitive area calculated by subtracting the A_{lumen} from the A_{true}

CoV: Coefficient of Variation

Table 3: Tensile properties before and after correction with FAF

	Mean Young's modulus (GPa)	Max. Young's modulus (GPa)	Average strength (MPa)	Maximum strength (MPa)
Using apparent diameter	7.35 \pm 1.95	12.0	91.2	157
With FAF = 2.982	21.9	35.8	272	467

FAF: Fiber area correction factor

Table 4 Comparison of the different areas on the same fibers

SAMPLE n.	A_{true} (μm²)	A_{def} (μm²)	A_{lumen} (μm²)	Lumen %
1	4732	3984	747	15.79
2	6219	5357	862	13.86
3	4918	3805	1113	22.63
4	4367	3760	607	13.89
5	3586	3161	426	11.87
6	4397	3930	467	10.63
7	7525	6362	1162	15.45
8	8602	7077	1525	17.73
9	4927	4213	714	14.50
11	4734	4162	572	12.09
12	8673	7965	708	8.16
13	4864	4146	718	14.76
14	6164	5270	894	14.50
15	5832	5103	729	12.50
16	5344	4600	744	13.93
17	4469	3770	699	15.64
18	4990	4442	548	10.98
20	4268	3387	881	20.64
21	5486	4492	994	18.12
22	4043	3293	750	18.54
23	5876	4861	1015	17.27
24	3906	3360	546	13.98
25	6950	5853	1097	15.79
Mean	5429	4624	805	14.92
StDevP	1366	1210	252	3.22
CoV (%)	25.16	26.17	31.29	21.58

A_{true} (μm²): True area calculated on ImageJ binary images of the CSA

A_{def} (μm²): Definitive area calculated by subtracting the A_{lumen} from the A_{true}

A_{lumen} (μm²): Lumen area

Lumen %: Lumen percentage in the A_{true}

StDevP: Standard Deviation

CoV: Coefficient of Variation

Table 5 Comparison with other studies in literature

Fiber	d (μm)	SD	CSA (μm ²)	SD	L (%)	SD	E (GPa)	SD	References
BF (leaf)	150.00	-	-	-	-	-	29.75	8.56	Pothan, Oommen and Thomas 2003
BF (leaf)	120.00	5.80	-	-	-	-	20.00		Idicula, Malhotra, Joseph and Thomas 2005
BF (peel)	113.90	13.75	5429	1366	14.92	3.22	7.35	1.95	-
Bagasse	399.05	76.75	-	-	-	-	-	-	Justiz-Smith, Junior Virgo and Buchanan 2008
Coir	396.98	67.93	-	-	-	-	-	-	Justiz-Smith, Junior Virgo and Buchanan 2008
Sisal	-	-	-	-	15,00	-	24.00	6.00	Oksman et al. 2002
Sisal	205.00	4.30	28733	5302	-	-	20.20	3.60	Thomason et al. 2011
Flax	-	-	9431	1231	-	-	50.00	7.50	Thomason et al. 2011
Jute	58.80	14.60	-	-	-	-	28.30	8.80	Virk, Hall and Summerscales 2009
Jute	-	-	-	-	33,96	-	-	-	Alves Fidelis et al. 2013

d: Diameter of the fiber

SD: Standard deviation

CSA: Cross-sectional area

L: Lumen ratio

E: Young's Modulus